Automated and Robust PERCIST-based Thresholding framework for whole body PET-CT studies

Lei Bi, Jinman Kim, *Member, IEEE*, Lingfeng Wen, *Member, IEEE* and David Dagan Feng, *Fellow, IEEE*

***Abstract*— Positron emission tomography (PET) is unique for quantitatively assessing treatment response before marked morphological changes are detectable by Computed Tomography (CT). PET response criterion (PERCIST) is a widely accepted approach of assessing metabolic response of malignant lesions by using Standardized uptake value (SUV) normalized by lean body mass (*LBM*) with a volume of interest (VOI) reference defined in the right lobe of liver. However, the operator-dependent delineation of VOI reference is a time consuming and subjective task. Although the VOI reference can be estimated from the co-aligned CT, the low-dose CT data in PET-CT poses challenge in liver segmentation. In this study, we propose a fully automatic framework to calculate the PERCIST-based thresholding for whole-body PET-CT studies. The framework consists of multi-atlas registration and voxel classification for CT data to segment liver structure and delineate the VOI reference, which is then mapped to the PET data to derive the value of SUV_{LBM} thresholding for PET to select regions of high metabolism. We evaluated our framework with 28 clinical studies diagnosed with lung cancer or lymphoma, and demonstrated both reliability and efficiency in depicting lesions using PERCIST thresholding.**

I. Introduction

In-vivo metabolic information, such as glucose metabolism, can be noninvasively visualized by positron emission tomography (PET) through administrating radioactive tracer into the human body. This facilitates diagnosis and assessing treatment response of cancer. Standardized uptake value (SUV), which is normalized by administrated tracer dose and patient body weight, has been widely accepted to provide approximate estimation of glucose metabolic rate for identifying malignant lesions by using FDG, a common radiopharmaceutical used in PET modalities. However, many factors affect the accuracy of SUV values, such as patient's size, uptake time, and glucose concentration. The use of lean body mass (*LBM*) or body surface area has been presented to provide more accurate estimation of body volume compared with body weight [1]. Thresholding has been widely used in the analysis of PET data, which classifies metabolic regions higher than a given 'threshold' value, so as to identify malignant lesions and regions with high metabolism. Efforts have been made to improve traditional thresholding with one constant value of thresholding, such as adaptive thresholding calculation that is dependent on local image attributes [2].

The most unique benefit of PET is to quantitatively assess treatment response before marked morphological changes are detectable by computed tomography (CT). PET response criterion (PERCIST) is a widely recognized measure of assessing metabolic response of malignant lesions. It suggests a thresholding method based on the combined use of SUV_{LBM} and volume of interest (VOI) reference, a 3cm diameter sphere, placed on the right lobe of the liver to measure the PET uptakes. In the case of abnormalities in the liver, the aorta can be used instead. These two structures were considered to be stable among the PET study population [3]. However, the delineation of the VOI reference in the liver and the subsequent thresholding calculation for malignant lesions is operator-dependent and time consuming. The automation of such the PERCIST-based thresholding would deliver great benefit and objective evaluation of treatment response especially when multiple sequential studies involved.

The main requirement for the automation of PERCIST thresholding is the segmentation of the VOI reference. There are a number of researches on liver segmentation for CT studies. Statistical shape model (SSM) algorithm was identified to be most accurate, but other approaches such as region growing and atlas-based algorithms demonstrated their advantages [4]. Multi-atlas based registration was also presented with the benefit of minimizing the error introduced by mis-registration from a single atlas method [5]. In whole-body PET-CT scanner, low-dose CT protocol is usually used, which results in low-contrast and high noise CT studies. However, the atlas based probabilistic segmentation was still found to be promising to segment liver from low-dose CT data in PET-CT studies [6].

Thus, in this study, we proposed a fully automated framework of PERCIST based thresholding calculation for whole-body PET-CT studies. Multi-atlas based segmentation approach will be employed in our solution for the liver estimate, which will be used in PERCIST later. Since the VOI reference is only a small subset of the liver, our liver segmentation algorithm was optimized to be reliable and robust to accommodate for large patient population variability and the low-dose CT in our PET-CT studies, where the low-dose CT limited our ability to differentiate the liver from other neighbouring structures based on the Hounsfield Units (HU) alone as exemplified in Fig. 2 and in [6]. For the training data, 10 whole body PET-CT studies with lymphoma were used to construct multi-atlases of the liver. The performance of the proposed framework was evaluated by 28 whole body PET-CT studies with lung cancer or lymphoma.

Lei Bi, Jinman Kim, Lingfeng Wen, and David Feng are with the School of Information Technologies, University of Sydney, Australia. Lei Bi (e-mail: lebi8696@uni.sydney.edu.au); Jinman Kim (phone: +61 2 9036 9708; fax: +61 2 9351 3838; e-mail: jinman.kim@sydney.edu.au).

Lingfeng Wen is also with Department of PET and Nuclear Medicine, Royal Prince Alfred Hospital, Australia (e-mail: wenlf@ieee.org).

David Dagan Feng is also with CMSP, Department of EIE, Hong Kong Polytechnic University, Hong Kong, and Med-X Research Institute, Shanghai Jiao Tong University, China (e-mail: david.feng@sydney.edu.au).

This research was funded in part by ARC grants.

II. Methods and Materials

A. Overview of the Proposed Framework

Fig.1 illustrates the overview of our framework. The proposed framework involves the use of anatomical information in co-registered CT data to coarsely segment the liver and delineate the VOI reference; the VOI reference is then used in the co-aligned PET counterpart, together with SUV_{LBM}, to derive the PET thresholding value.

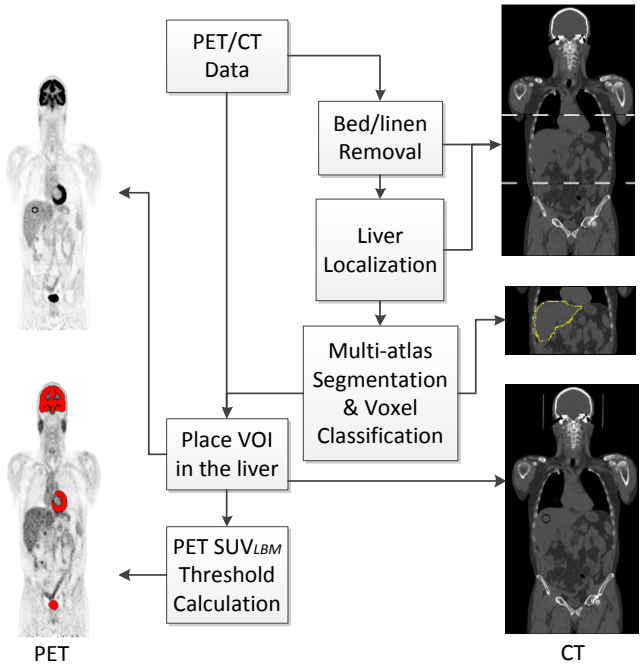

Figure 1. Overview of our proposed framework for the automated PERCIST-based thresholding calcualtion with PET-CT studies. Note that due to the nature of PET-CT acquisition, the right side of the body is depicted on the left side of these images.

B. Patient Data

All the PET-CT studies were conducted at a Siemens Biograph TruePoint PET-CT scanner in the department of PET and Nuclear Medicine, Royal Prince Alfred hospital. All the studies have 326 slices with slice thickness of 3 mm to cover the whole body from top head to upper thigh with PET slice size of 200×200 at pixel size of 4.07 mm^2 and CT slice size of 512×512 at the pixel size of 0.98 mm^2. The evaluation data consists of 20 studies of 20 patients for the staging of non-small cell lung cancer and 4 sequential studies of 2 patients for the treatment response of lymphoma. In addition, 10 whole body studies of 10 patients diagnosed with lymphoma were used as the training data. No abnormalities were observed in the liver for all the studies.

C. PET-CT Pre-processing

The CT images were initially pre-processed to remove the background and the scanner bed/linen automatically by adaptive thresholding and image subtraction from a bed template [7]. The value of *LBM* was then derived according to [8] and convert PET data to SUV_{LBM} map:

$$LBM(kg) = weight - \{weight \times [(1.2 \times weight / height^2) + 0.23 \times age - 10.8 \times Gender - 5.4] / 100\} \quad (1)$$

where Gender = 1 for male and 0 for female. Weight, height and age are expressed in kilograms, meters and years respectively.

D. Constructing Multi-atlases of Liver

Multi-atlases of liver for CT data were constructed with a CT volume and corresponding liver segmentation (label) pair, by semi-automatically segmenting 10 PET-CT studies with healthy liver (training data) using the liver segmentation module in the medical imaging interaction toolkit (MITK) [9]. To ensure that the liver was correctly identified for the low-dose CT data, under-segmentation of the liver was preferred for uncertain parts of liver. From the training data, voxel level features were extracted for voxel classification with intensity, Gaussian derivatives, gradients, and the voxel's 3D location index measured according to the percentage of the segmentation label being above, next or behind the voxel [10]. All these features were then normalized to the range [0, 1] by linearly scaling non-angle features to a random variable with zero mean and unit variance, and shifting the value so that it was within the desired range [11].

E. Liver Segmentation

1) Liver Localization

The lung structure was initially segmented from CT data based on [12] to initialize the location of the liver. From the whole-body CT data, an adaptive thresholding method was applied to separate the low intensity air tissue from other tissues according to the value of CT data. The two largest segmented regions were extracted as the lung by using region growing algorithm.

Using the segmented lungs to estimate the first top slice of the liver, we defined the liver subsection to be 60 slices (based on the average liver volume size from our training data) supplemented by 30% (18 slices) above and 10% (6 slices) below to our estimated liver.

2) Multi-atlas based Liver Segmentation and Voxel classification

Firstly, the 10 liver atlases (training data) were warped to the sample data space (after liver localization) for a given PET-CT studies by using the Elastix package with the affine translation and BSpline elastic registration [13]. The optimal CT liver registration parameters were set based on the estimates in [10]. The CT volumes were then transformed by using the derived transformation parameters to transfer the liver labels from the atlases to the given CT volume. The transformed labels from multi-atlases of liver were then concatenated into a single label, where only 50% of the commonly registered area was kept such that voxels comprising of high correlation among the registered atlases are retained.

As shown in Fig. 2, the obtained volume of the liver was expanded by 30 voxels to compensate any under-segmentation that may occur through the multi-atlas registration. The K-nearest neighbor (KNN) classifier [10]

was then applied to all the voxels in the expanded label to classify whether the voxel belong to the liver, measuring the probability of each voxel using a statistical classifier and features. In our study, we set $K=15$ and the features defined in Subsection D. were used with Euclidean distance measures.

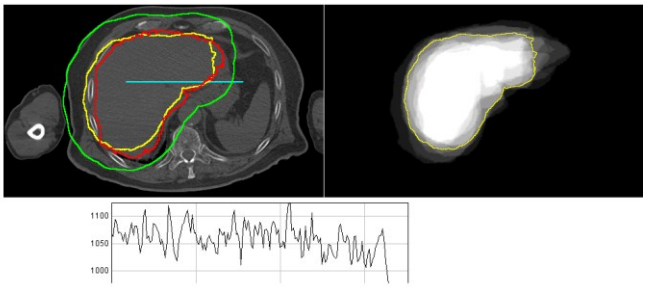

Figure 2. An axial slice of a liver (left) with its segmented result. The yellow outline is the result from the multi-atlas registration (right), the green outline is the 30 voxel extension which were used in the voxel classification resulting in the red outline as the liver segmentation. A line profile (bottom) generated from blue line, illustrates the difficulty in the segmentation where the HU values cannot be differentiated from the liver to its neighbor structure.

3) VOI Reference Segmentation

From a slice located at 40% of the total segmented liver labeled slices, we reduced the label outline by 30 voxels with an erosion filter. The top-right corner from the reduced label was then used to calculate the VOI reference. This ensured that the VOI of 3cm diameter was completely within the right lobe of the liver.

F. PERCIST-based Thresholding for PET SUV_{LBM} Data

The VOI reference from CT was used to derive the values of thresholding *Th-*SUV_{LBM} according [14]:

$$Th\text{-}SUV_{LBM} = (1.5 \times Mean) + (2 \times SD) \quad (2)$$

based on the mean and the standard deviation (SD) of the voxels in the segmented VOI reference. This derived value was used to evaluate the PET studies, as exemplified in Fig. 3.

III. Results and Discussions

A. Liver Segmentation and VOI Reference for CT data

In this study, we considered the right lobe to be the right half of the PET liver. This is a conservative estimate ensuring the selection of voxels belongs to the right lobe. Experiment with 28 PET-CT studies showed the derived VOI references were correctly defined in the right lobe and away from the boundary by visual interpretation from two experienced operators. Fig. 4 shows examples of automated liver segmentation and the VOI reference.

Among the 28 studies, the accuracy of the liver segmentation varied with expected over-estimation occurring when the liver was touching adjacent structures, shown in Fig. 4(b) and 4(d) (most noticeable in the coronal views). Nevertheless, our liver estimates were found to be robust in the calculation of the VOI references.

We used 10 training data to construct the atlases. This was found to be sufficient; however, we will investigate the effect from larger training data which will cover greater variations of individuals.

B. Thresholding of PET data

The VOI references segmented above were used in the thresholding calculation in the PET counterpart. As a further test to the accuracy of the VOI reference segmentation, we measured the homogeneity of the voxels residing in the VOI in PET, where if the VOI is entirely in the liver, it is expected to be homogeneous and thus have low SUV_{LBM} standard deviation from the mean. In average, we calculated the 1st order standard deviation to be within 14.56% (±2.99%) to the mean SUV_{LBM}, which was within the expected variation of SUV_{LBM} found in the liver structure from our experiments. Fig. 3 illustrates an example of using the VOI reference in the calculation of SUV_{LBM} thresholding for a sequential of studies in the treatment response assessment for a patient with a high-grade lymphoma. The results of the adaptive SUV_{LBM} thresholding were able to depict all the abnormalities for multiple studies, which were consistent to the findings in the physician's reports.

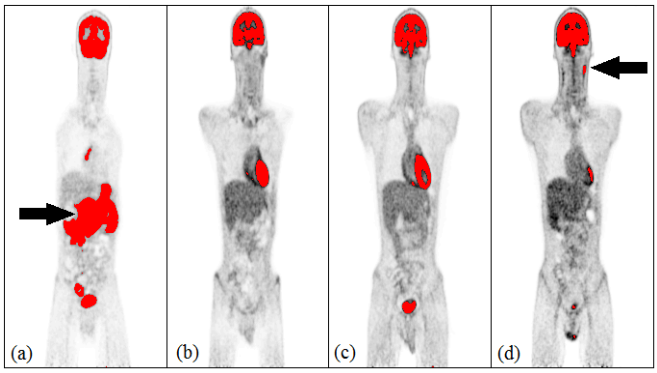

Figure 3. (a) Primary staging of lymphoma with immeasurable spread throughtout the body; (b) and (c) shows good response from treatment; and (d) shows moderately increased glucose metabolism in lymph nodes on the neck area (indicated by an arrow). The images were manually aligned to relative view of the body. The automated thresholding was able to depict all the abnormalities, together with noramlly occuring uptakes in the brain, bladder, kidney and heart, which was consistent to the expert assessment in our clinical reports.

C. Computational Cost

The full process took in average of 125.0 ± 19.2 min for a PET-CT study (326 slice pairs) running on a standard PC with a 2.5GHz dual core CPU and 6GB RAM. The time consuming tasks were the atlas-registration (~20% of total time) and voxel classification of liver (~77% of total time). In the registration, for each sample, we used 10 atlases thus requiring high computation. As for the classification, we used 500,000 training voxels derived from our 10 training data to ensure that maximum variations of the voxels were represented. This resulted in more than half million comparisons for each voxel in the sample volume. Since our current study was aimed at validating the reliability of our framework, the computational efficiency will be improved in our future study by sample reduction and code optimizations.

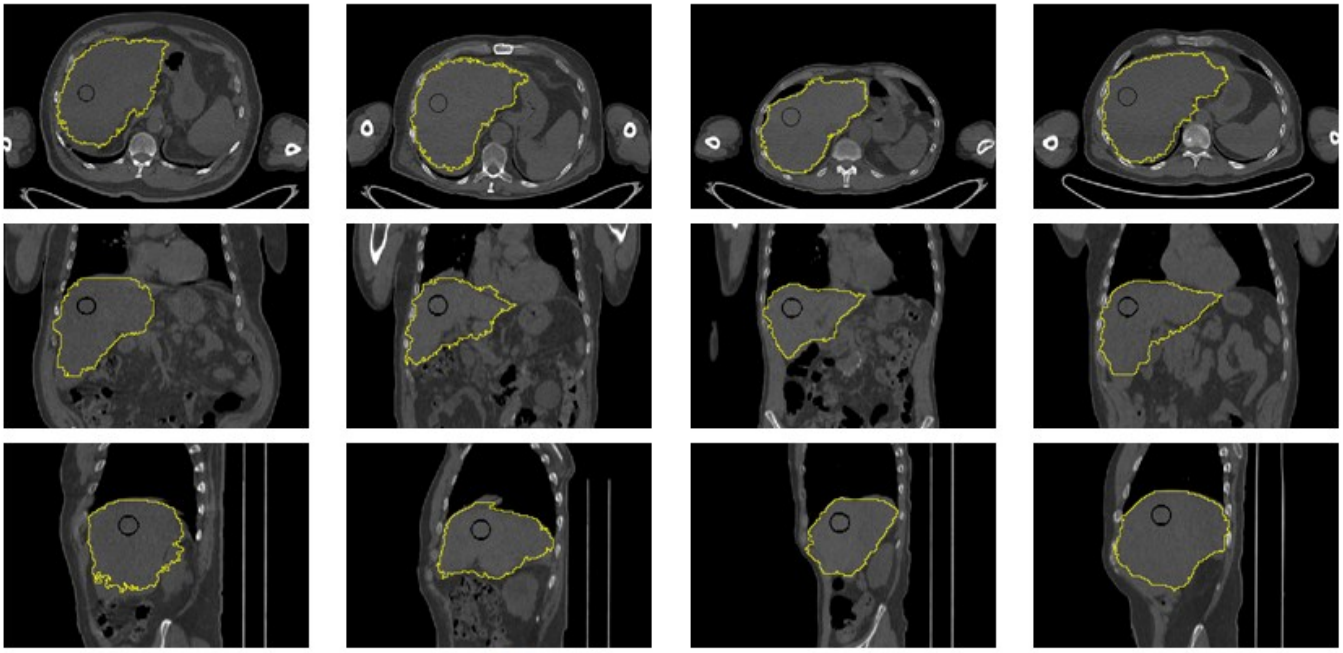

Figure 4. VOI reference segmentation results on 4 patient studies (columns) in axial (top), coronal (middle) and saggital views (bottom). The yellow boundary is the result of the liver estimate which were used in the calculation of the VOI references shown as black circles.

IV. Conclusion and Future Work

In this study, we developed a fully automatic reliable and robust framework for PERCIST-based thresholding for whole-body PET-CT studies. Our results demonstrated the reliability of our liver segmentation using multi-atlas registration for low-dose CT data in PET-CT studies, and also in the calculation of the PERCIST thresholding value for detecting malignant lesions. In our future studies, we will investigate the inclusion of aorta segmentation to our framework to accommodate for PET studies with abnormal liver. We will also further evaluate the performance of our method as well as its application towards automated change detection in PET-CT studies to assess tumor response to therapy.

Acknowledgement

We like to thank our collaborators at the Royal Prince Alfred (RPA) hospital.

References

[1] D. Feng, et al., "Techniques for parametric imaging. In: Biomedical Information Technology," *Elsevier press: San Diego*, pp. 137-63, 2007.
[2] W. Jentzen, et al., "Segmentation of PET volumes by iterative image thresholding," *J. Nucl. Med.*, vol. 48, pp. 108-14, 2007.
[3] R.L. Wahl, et al., "From RECIST to PERCIST: evolving considerations for PET response criteria in solid tumors," *J. Nucl. Med.*, vol. 50, pp. 122S-50S, 2009.
[4] T. Heimann, et al., "Comparison and evaluation of methods for liver segmentation from CT datasets," *IEEE T. Med. Imag.,* vol. 28, pp. 1251-5, 2009.
[5] E. M. van Rikxoort, et al., "Adaptive local multi-atlas segmentation: Application to the heart and the caudate nucleus," *Med. Image Anal.,* vol. 14, pp. 39-49, 2010.
[6] C. Li, et al., "Automated PET-guided liver segmentation from low-contrast CT volumes using probabilistic atlas," *Comput. Meth. Prog. Bio,* in press, 2012.
[7] J. Kim, et al., "A fully automatic bed/linen segmentation for fused PET/CT MIP rendering," *J. Nucl. Med.*, 49(Suppl 1), 387P, 2008.
[8] R. Pieterman, et al., "Visualisation and assessment of the protein synthesis rate of lung cancer using carbon-11 tyrosine and positron emission tomography," *Eur. J. Nucl. Med.*, vol. 29, pp. 243-7, 2002.
[9] The Medical Imaging Interaction Toolkit. http://www.mitk.org/
[10] E. van Rikxoort, et al., "Automatic segmentation of the liver in computed tomography scans with voxel classification and atlas matching", *MICCAI segmentation workshop*, pp. 101-8, 2007.
[11] S. Aksoy and R.M. Haralick, "Feature normalization and likelihood-based similarity measures for image retrieval", *Patterm Recogn. Lett,* vol. 22, pp. 563-82, 2001.
[12] S. Hu, et al., "Automatic lung segmentation for accurate quantitation of volumetric X-ray CT images," *IEEE T. Med. Imag.,* vol. 20, pp. 490-498, 2001.
[13] S. Klein and M. Staring, Elastix. http://www.isi.uu.nl/Elastix/
[14] P. Ghosh et al., "Expanding the Power of PET with PERCIST", *Siemens Medical Solutions USA, Inc.,* 2010.